ANALYSIS AND SIMULATION OF THREE-DIMENSIONAL SCATTERING DUE TO HETEROGENEOUS CRUSTAL STRUCTURE AND SURFACE TOPOGRAPHY ON REGIONAL PHASES; MAGNITUDE AND DISCRIMINATION

Arben Pitarka[1], Don V. Helmberger[2], and Sidao Ni[1]

URS Group, Inc.[1] and California Institute of Technology[2]

Sponsored by Air Force Research Laboratory

Contract No. FA8718-07-C-0003[1,2]

ABSTRACT

The main purpose of this study is the basic understanding of scattering and its effects through step-by-step numerical experiments and waveform modeling, with the goal of providing useful insights into ongoing research for development of simple empirical models of scattering that can be used in reducing the scatter in measures of Lg and coda wave magnitude and for discrimination purpose as well. We are performing anelastic three-dimensional (3-D) finite-difference simulations of wave propagation in highly heterogeneous media for a range of source depths, receiver distances, and source types. Using a highly efficient and parallelized computer code and models with flat surface topography we have produced synthetic seismograms up to 3.5 Hz at regional distances up to 300 km. In future works we plan to extend the upper frequency limit to 6-8 Hz and model surface topography scattering effects by using a larger number of computer nodes. Our numerical experiments with 3-D velocity models that include random velocity perturbations and microbasins, designed to produce wave scattering in the upper 5 km of the crust, clearly show that wave-path scattering alone can produce Lg, P, and S coda waves with significant energy even for explosion sources. The energy of Lg coda waves depends on the source depth. P/Lg ratios estimated at different frequencies indicate that this ratio could be a good discriminant between explosions and earthquakes when calculated at high frequencies. P/Lg ratios below 1 Hz are very similar for shallow explosions and deep earthquakes.

OBJECTIVES

Our objective is to analyze and evaluate the effect of scattering on the amplitude and frequency content of Pg and Lg waves due to small-scale crustal heterogeneities and surface topography by 3-D finite-difference simulations and modeling of recorded waveform data. The research program will focus on the following topics:

1. Influence of scattering due to complex structure and surface topography on the variability observed in amplitude estimates of regional phases. We will analyze simulation results of regional wave propagation scattering, obtained with efficient two-dimensional (2-D) and 3-D finite-difference computer programs that can also treat surface topography, including mini-basins.
2. Influence of scattering effects due to rough topography near the source and station on the amplitude of observed regional phases involving explosion source. Topography analysis will be concentrated in small areas, mostly in Korean Peninsula, India, and Pakistan, where we have sufficient data on earthquakes and explosions.

RESEARCH ACCOMPLISHED

The influence of random heterogeneities and rough surface on Lg amplitude and Lg coda formation are shown to be significant. This very important phenomena needs to be investigated by both observational and numerical techniques. While analyses of recorded seismograms can reveal the degree of complexities in the crust and the effect of small-scale and large-scale perturbation on different wave phases, the numerical experiments can be used for isolating effects caused by the wave path, seismic source, and local structures. They can also be used to verify hypothesis that are at the foundation of several discrimination methodologies.

The regional discriminants and magnitude methods rely mainly on the general feature of decreased s-phase amplitude and increase of p-phase amplitudes for explosion sources. However explosions produce anomalous large s-phase amplitudes that confound regional methods. It is therefore important to understand the factors that are at the origin of such behavior. Several valid hypothesis dealing with the source process and crustal complexities have been proposed. In this study we investigate one of them—the effect of scattering due to random heterogeneities in the upper crust on the local and regional wavefield from explosion and earthquake sources.

Parameterization of Scattering Model

The wave scattering effects in our 3-D simulations are modeled by random perturbations of the velocity. The perturbations expressed in percentage of unperturbed shear-wave velocity are intercorrelated using a spatial correlation length. Results of sensitivity analyses with different velocity perturbations and correlation lengths, not shown here, confirm the importance of such modeling parameters in generating realistic wave-path effects in a broad frequency range. One way of deriving realistic scattering model parameters is to simulate observed broadband waveforms from small and moderate regional earthquakes using random perturbations of well calibrated velocity models. The objective of such modeling is to derive scattering parameterization of the velocity model by reproducing the gradual disappearance of the observed radiation pattern of P and S waves with increasing frequency. This is known to be caused by near-source and wave-path scattering. The use of both P and S waves as well as their respective coda decay provides excellent empirical constraints on deriving realistic random velocity perturbations with correct correlation lengths. The effect of wave scattering on P and S waves and their coda amplitude is illustrated in Figure 1.

Figure 1 shows the amplitude variation of the ground velocity envelope as a function of frequency from the Mw4.5 070120 earthquake in South Korea. We used broadband recordings at station CHC, CHJ, ULJ, and SES. The station and the earthquake locations are shown in Figure 2. The earthquake was located at a depth of 11 km. Its focal mechanism (strike=209^{o}, dip=90^{o}, rake=180^{o}) was determined using a cut and paste (CAP) inversion technique that is based on different weights for relatively high frequency waveform modeling of Pnl and relatively long period surface waves (Tan et al., 2006). And Pnl and surface waves are also allowed to shift in time to take account of uncertainties in velocity structure. Inversion of Pnl and surface waves provides better constraints on focal depth as well as source mechanisms. The pure strike-slip mechanism of the earthquake and its recording at stations near the P wave nodal planes are ideal for analyzing regional scattered waves. Stations CHJ and CHC are close to P-wave nodal planes.

Two general observations relevant to the wave scattering can be made. First, the P-wave scattering, expressed as the relative increase of amplitude of the P wave and its coda in the tangential component of motion at P-wave nodal stations, becomes significant at frequencies higher than 4 Hz. Note the relatively large amplitude of P coda waves on the tangential component at such frequencies. This indicates that high-frequency P to S-wave conversions are significant. It is important to note that scattering effects due to small-scale perturbation in the shallow crust cause the increase in amplitude of high frequency P-wave coda in all three components. P waves also could be very helpful in constraining the basic parameters of the scattering model. Second, because of their shorter wavelength S waves are more susceptible to wave propagation scattering effects. As shown in Figure 1, for such waves the amplitude difference between the three components that is controlled by the source radiation pattern is observed only at frequencies lower than 2 Hz. In general, at higher frequencies the amplitude of the S wave coda is mainly controlled by scattering. Consequently it is the same for all three components. The relatively low frequency random behavior of S waves can be used in deriving random variations in the crustal velocity model. This observed feature of P and S phases can help constraining scattering parameterization. In our ongoing effort for deriving scattering parameterization for the Korean Peninsula we will model several shallow earthquakes recorded at regional broadband stations.

The ratio between Pn and Pg seems to be stable over different frequencies. For strike-slip events such as the 070120 Korean earthquake, Pn should be much smaller than Pg because of its steeper takeoff angle. But for explosions, Pn and Pg seem to have similar amplitudes (Kim and Richards, 2007). For the Korean earthquake, Pn is indeed much weaker than Pg for all the frequency bands, arguing that the ratio between Pn and Pg can be used to constrain source mechanisms of events at high frequencies and should be very useful for discrimination purposes.

Modeling 3-D Scattering Effects

The origin of the high frequency scattering affecting mainly the P and Lg coda waves (above 1 Hz) could be due to either deep or shallow crustal structure complexities along the wave path or in the source region (e.g., Dainty 1996; Wu et al., 2000). The Lg wave shows evidence of scattering from small-scale structures. Other causes of scattering could also be large-scale structural complexities such as crustal thinning or multipathing (e.g., Ni and Barazangi, 1983; Phillips et al., 2000).

During this first phase of our study we have examined effects of wave propagation scattering due to complexities in the shallow crust. We have calculated synthetic seismograms for point sources buried at different shallow depths using a parallelized anelastic 3-D finite-difference code (Pitarka, 1999). Our finite difference code solves the stress-velocity wave equations in a heterogeneous medium using staggered grids. The technique for generating the 3-D velocity model on a regular grid with variable spacing allows for inclusion of small-scale complexities and surface topography as well. The technique we use to model free surface topography is an extension of the formalism that we have applied to modeling wave propagation in media with curved free surface (Pitarka and Irikura, 1996). The performance of our free-surface boundary condition technique at handling Lg coda waves for flat free surface and very long distances was compared with that of the FK method of Saikia (1994) for a shallow source. Also the technique has been validated against other standard and accurate techniques for modeling surface topography such as 2-D-Boundary Element Method (BEM) and the 2-D-Discrete Wavenumber-Boundary Integral Equation method of Takenaka et al. (1996).

We looked at the relative contribution of wave-field scattering on different frequency bands of P and Lg coda waves due to localized and highly heterogeneous small-scale bodies embedded in a reference planar layered velocity model that was used in modeling regional wave propagation in the South Korea region. The small-scale variations of the velocity are randomly distributed along the top 5 km of the crust. In addition to the small-scale fluctuations our velocity model includes several microbasins with sizes varying between 10-25 km and depth up to 2 km. The velocity fluctuations are in the range of 2-8% and their correlation length is 5 km. The selected minimum grid spacing of 200 m ensures accurate wave propagation modeling up to 3.5 Hz. The 3-D model occupies a volume of 400x200x60 km. The ground motion velocity was computed on a 2-D rectangular array of stations located on the free surface. The stations spacing is 20 km, and the maximum epicentral distance is 300 km. Several stations are located in the microbasins.

Aiming at understanding scattering effects in relation with the source type and source depth we performed simulations for an explosion point source located at a depth of 500 m, and for earthquake double-couple point sources located at 50 m and 8 km depths, respectively. Since we are looking at indirect mechanisms of S wave generation, mainly wave-path scattering, in our simulations we used the isotropic representation of the explosion source.

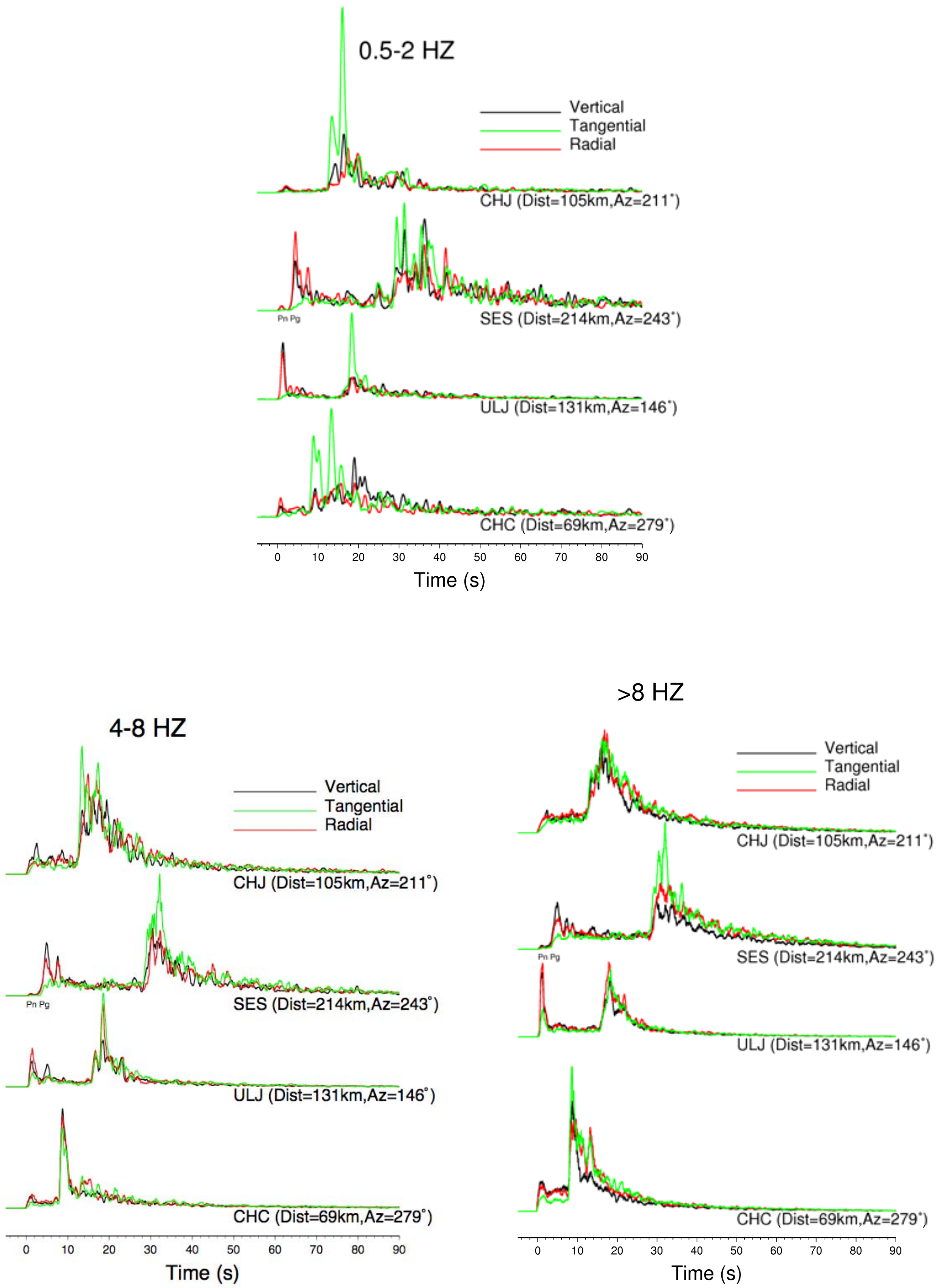

Figure 1. Smoothed envelopes of broadband velocity seismograms recorded at station CHJ, SES, ULJ, and CHC from the Mw 4.5 070120 earthquake in South Korea. The envelopes are calculated at four frequency bands indicated on top of each panel. Color traces show different components. The epicentral distance and azimuth are indicated at each trace. Note the large amplitude of the P wave on the vertical and radial components at stations CHJ, SES, and ULJ that are located near the nodal planes. The difference in the P wave seen between the three components is caused by the source radiation. It is preserved only at frequencies up to 4 Hz. In general, at frequencies higher than 4 Hz, the amplitude of P wave coda becomes the same at all components. This is a clear indication of scattering effects in the shallow crust.

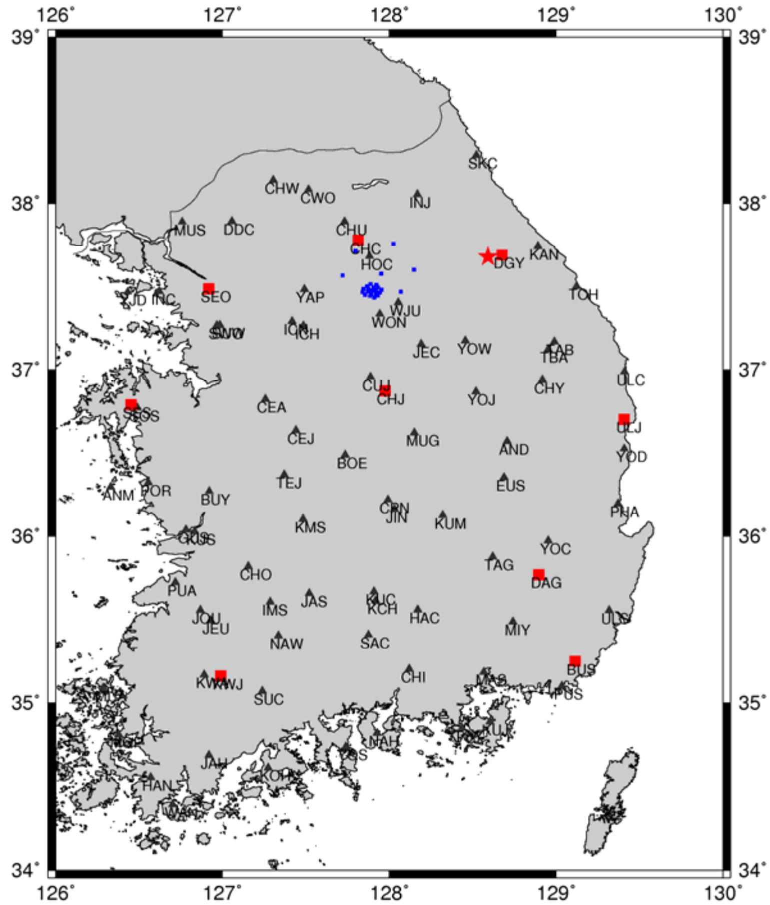

Figure 2. Map showing broadband (red square) and short-period strong motion (black triangle) stations in South Korea. Blue squares show International Monitoring System Korean Seismic Research Station (KSRS) stations, and the red star indicates the epicenter of the earthquake analyzes in this study.

The source time function is a modified Haskell type:

$$\psi(\tau) = \psi_\infty \left[1 - e^{-K\tau} \left[1 + K\tau + \frac{(K\tau)^2}{2} - B(K\tau)^3 \right] \right] \tag{1}$$

where τ is the reduced time. The study by Mueller and Murphy (1971) established the basic scaling laws relating the constant K and ψ_∞ to yield. The parameter K is directly related to the corner frequency, and depends on source strength such that the larger the event, the longer is the source duration, or

$$K = C_1 \frac{h^{0.42}}{W^{0.33}}, \tag{2}$$

where W is the yield in kt, h is the depth in meters, and C_1 is a constant determined by near-field modeling.

Simulation Results

Figure 3 shows the difference in wave propagation characteristics between the reference flat-layered model and the 3-D model with shallow crustal scattering. We compared the E-W component of synthetic velocity seismograms calculated at a linear array of receivers for a strike-slip earthquake located at a depth of 8 km. The strike angle of the fault is 90^{o} and the rake angle is 50^{o}. It is obvious that shallow random complexities create coda waves with long duration. The S and Lg coda waves are very energetic even at short distances.

Figure 4 compares the synthetic waveforms from a shallow isotropic explosion source buried at a depth of 0.5 km and a double couple point source with an arbitrary focal mechanism located at a depth of 8 km. Again the effects of the shallow heterogeneities expressed as P to S and S to P conversions as well as surface waves are very impressive, especially for the explosion source that does not emit S waves. Our numerical experiment clearly shows that wave-path scattering alone can produce Lg, P, and S coda waves with significant energy even for shallow explosion sources. Other simulations performed with the same scattering model confirm that the energy of Lg coda waves increases when the source depth decreases. An even more drastic effect can be expected for rough topography.

Using the waveforms from the shallow explosion source and deep earthquake source using the 3-D scattering model we estimated the P/Lg ratio at 0.5 Hz, 1 Hz, and 2 Hz. The P/Lg ratio was estimated at 95 receivers. The time window used for the P wave includes the direct P and P coda waves. The ratio at each frequency was obtained by averaging over a 0.5 Hz long frequency window centered at the required frequency. The comparison of P/Lg ratio between the explosion and earthquake is shown in Figure 5. Our result shows that for structures with shallow wave-path scattering P/Lg ratio at 2 Hz could be a good discriminant between explosions and earthquakes. P/Lg ratios below 1 Hz are very similar for shallow explosions and deeper earthquakes.

The difference of P/Lg ratio between the explosion and the deep earthquake at high frequency is controlled by the P rather than Lg waves. As demonstrated by our simulation the energy of Lg coda waves for both shallow explosion and deep earthquake sources is very similar. At longer distances P waves generated by the shallow explosion become richer in high frequency energy compared with the P waves coming from the earthquake source (see Figure 6). This is probably because for shallow sources P and converted P to S waves remain trapped within the scattering structure of the shallow crust. In contrast P waves coming from a deeper source, besides being attenuated, do not develop much coda waves as some of their energy reflected at the free surface leaks back to the deeper crust.

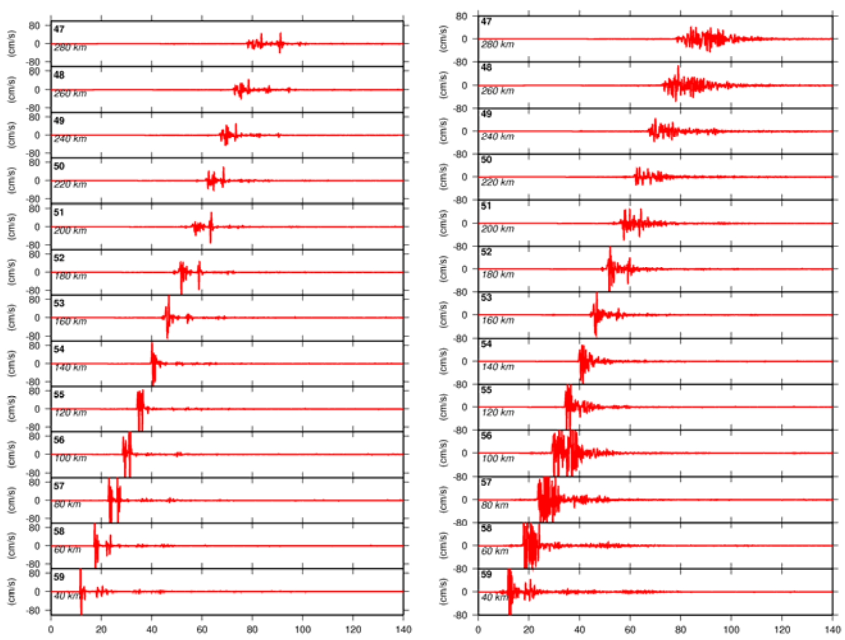

Figure 3. **Comparison of the E-W component of synthetic velocity seismograms calculated at a linear array of receivers, for a strike-slip earthquake located at a depth of 8 km. The receiver number and distance is indicated on each panel. The synthetics shown on the left panel are calculated with a reference flat-layered model, and the ones on the right panel are calculated with a 3-D model that includes shallow crustal scattering effects.**

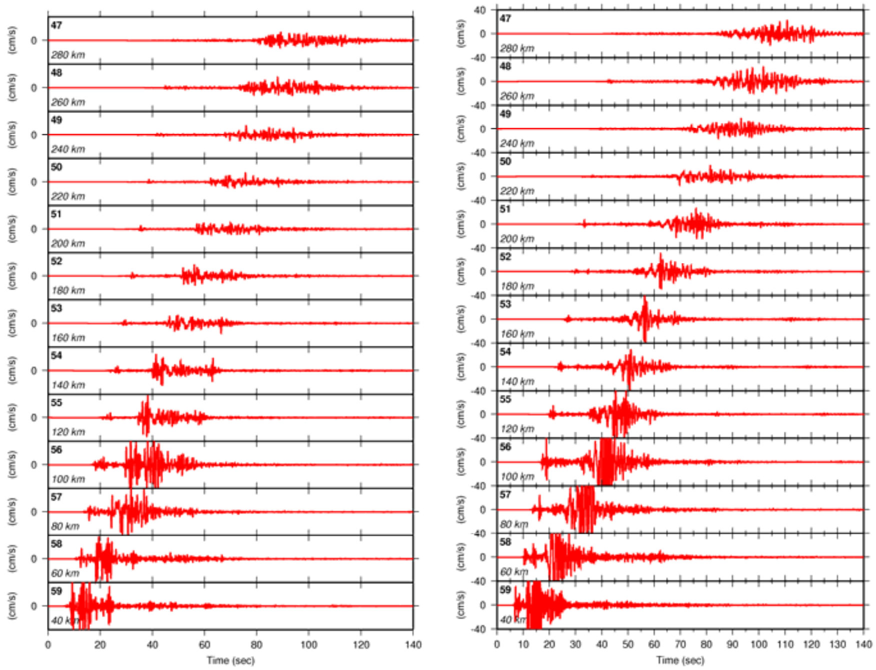

Figure 4. Vertical component of synthetic velocity for an earthquake with arbitrary focal mechanism and source depth of 8 km (left panel) and isotropic explosion source at a depth of 0.5 km (right panel). The synthetic seismograms are calculated with a 3-D model that includes shallow crustal scattering effects. Note the impressive energy of S and Lg coda waves developed for an explosion source.

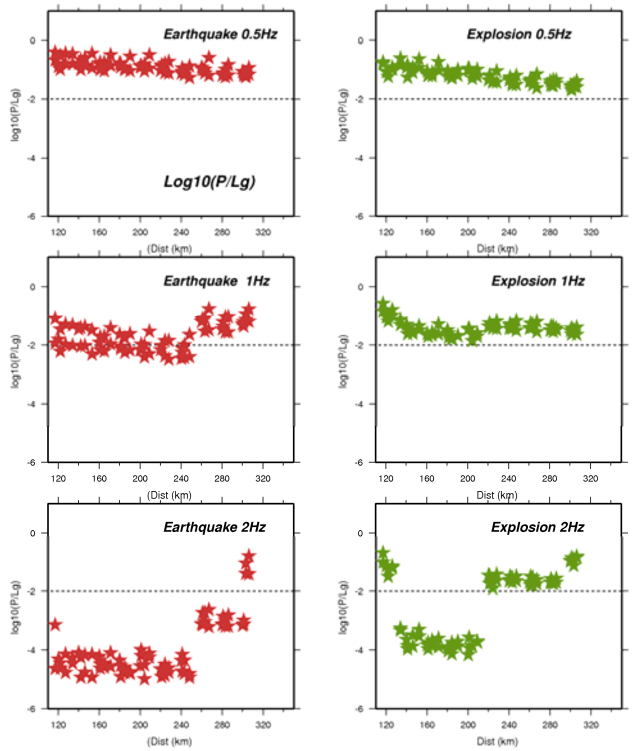

Figure 5. P/Lg ratios calculated at different frequencies for an earthquake at a depth of 8 km (left panels) and an isotropic explosion source at a depth of 0.5 km (right panels). For this case P/Lg calculated at the 2 Hz ratio can be considered as a discriminant at distances longer than 200 km.

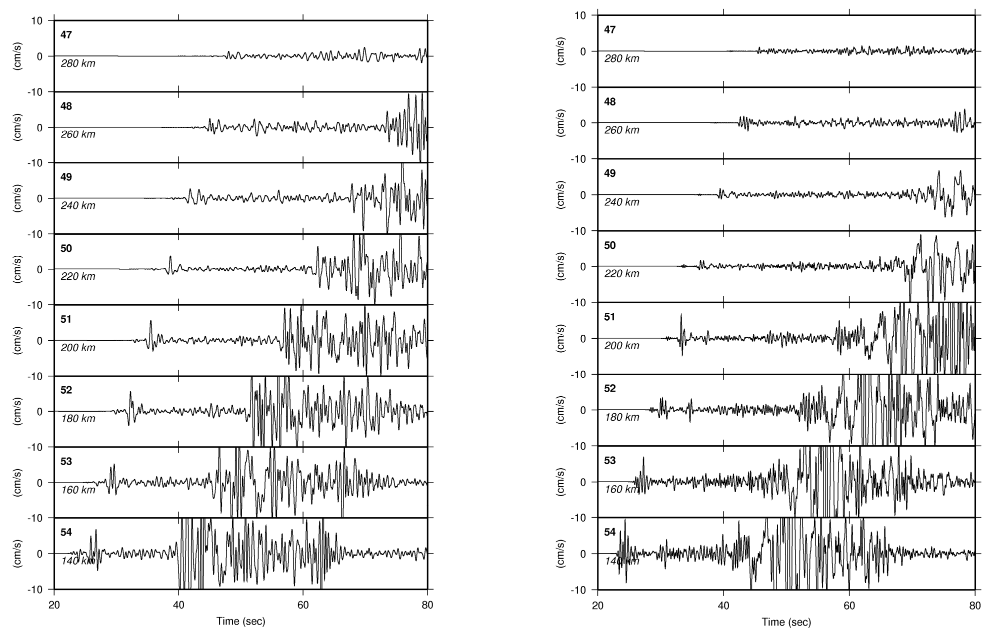

Figure 6. **Vertical component of the P wave part of synthetic seismograms calculated for the earthquake (left panel) and shallow explosion (right panel). Note the explosion contains higher-frequency P coda waves.**

CONCLUSIONS AND RECOMMENDATIONS

Our numerical experiments with 3-D velocity models that include random velocity perturbations and microbasins, representing wave scattering in the upper 5 km of the crust, clearly show that wave-path scattering is a major contributor to S and Lg coda waves from explosions. The energy of Lg coda waves depends on the source depth. P/Lg ratios estimated at different frequencies indicate that this ratio could be a good discriminant between explosions and earthquakes when calculated at high frequencies. P/Lg ratios below 1 Hz are very similar for shallow explosions and deeper earthquakes.

REFERENCES

Dainty, A. (1996). The influence of seismic scattering on monitoring. *Monitoring a Comprehensive Test Ban Treaty*. E. S. Husebye and A.M. Dainty, 663–688.

Goff, J. A., and T. H. Jordan (1988). Stochastic modeling of seafloor morphology: Inversion of sea beam data for second-order statistics, *J. Geophys. Res*. 93: 13589–13608.

Kim, W. and P.G. Richards (2007). North Korean Nuclear Test: Seismic Discrimination at Low Yield, *Eos Trans. Am. Geophys. Union*, Volume 88, Issue 14, p. 158–161.

Mayeda, K. M., A. Hofstetter, J. L. O'Boyle, and W. R. Walter (2003). Stable and transportable regional magnitudes based on coda-derived moment rate spectra, *Bull. Seism. Soc. Am*. 93: 224–239.

Mueller, A., and J. R. Murphy (1971). Siesmic characteristics of underground nuclear detonations, *Bull. Seism. Soc. Am.* 6: 1675–1692.

Myers, C. S., J. Wagoner, L. Preston, K. Smith, H. Tkalcic, and S. Larsen (2006). The effect of realistic geologic heterogeneity on local and regional P/S amplitude ratios based on numerical simulations, in *Proceedings of the 28th Seismic Research Review: Ground-Based Nuclear Explosion Monitoring Technologies,* LA-UR-06-5471, Vol. 1, pp. 146–155.

Ni, J. and Barazangi, M. (1983). High frequency seismic wave propagation beneath the Indian shield, Himalayan Arc, Tibetan Plateau, and surrounding regions: high uppermost mantle velocities and efficient Sn propagation beneath Tibet, *Geophys. J our. Roy. Astron. Soc*. 72: 655–689.

Phillips, W.S. and K. Aki (1986). Site amplification of coda waves from local earthquakes in central California, *Bull. Seism. Soc. Am*. 76: 627–648.

Phillips, W. S., H. E. Hartse, S. R. Taylor, and G. E. Randall (2000). 1 Hz Lg Q tomography in central Asia, *Geophys. Res. Lett*. 27: 3425–3428.

Pitarka, A. (1999). 3D elastic finite-difference modeling of seismic motion using staggered grid with nonuniform spacing, *Bull. Seism. Soc. Am*. 89: 54–68.

Pitarka, A. and K. Irikura (1996). Modeling 3D surface topography by finite-difference method: Kobe-JMA station site, Japan case study. *GRL* 20: 2729–2732.

Saikia, C.K. (1994). Modified frequency-wave-number algorithm for regional seismograms using Filon's quadrature-modeling of L(g) waves in eastern North America, *Geophys. J. Int*. 118: 142–158.

Takenaka, H., B.L. Kennett and H. Fujiwara (1996). Effect of 2-D topography and 3-D seismic wave field using a 2.5-D discrete wavenumber-boundary integral equation method, *Geophys. J. Int*., 124(3), 741-755.

Wu, Ru-Shan, S. Jin, and Xiao-Bi Xie (2000). Seismic wave propagation and scattering in heterogeneous crustal waveguides using screen propagators: I SH-waves, *Bull. Seism. Soc. Am*. 90: 401–413.

Tan, Y., L. Zhu, D.V. Helmberger and C.K. Saikia (2006). Locating and modeling regional earthquakes with two stations, *J. Geophys. Res.* 111: B01306, doi:10.1029/2005JB003775.

Xie, X., T. Lay and R. Wu (2005). Near-source energy partitioning for regional waves in 2D and 3D models, contributions of S^*-to-Lg and P-to-Lg scattering, in *Proceedings of the 27th Seismic Research Review*: *Ground-Based Nuclear Explosion Technologies,* LA-UR-05-6407, Vol. 1, 249–258.